Support Information (SI)

Obtaining High Mechanical Performance Silk Fibers by Feeding Purified Carbon Nanotubes/Lignosulfonate composite to Silkworms

Hao Xu[1,2], Wenhui Yi[1,2], Dongfan Li[3], Ping Zhang[1,2], Sweejiang Yoo[1,2], Lei Bai,[1,2] Jin Hou[4], Xun Hou[1,2]*

[1]Department of Electronic Science and Technology, School of Electronics and Information Engineering, Xi'an Jiaotong University, Xi'an 710049, P.R. China

[2] Key Laboratory for Physical Electronics and Devices of the Ministry of Education &Shaanxi Key Laboratory of Photonics Technology for Information, Xi'an Jiaotong University, Xi'an 710049, P.R. China

[3] Frontier Institute of Science and Technology, Xi'an Jiaotong University, Xi'an 710054, P.R. China

[4] Xi'an Medical University, Department Pharmacology, School Basic Medical Science, Xian 710021, P.R. China

* Corresponding authors: yiwenhui@mail.xjtu.edu.cn

1. Supplementary Figures S1–S5

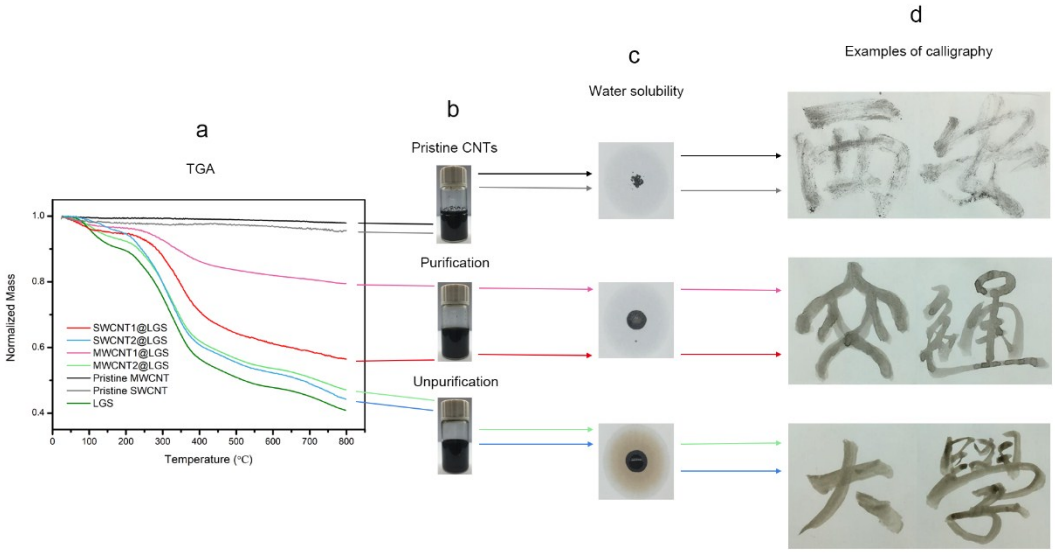

Figure S1. Characterization and illustration of artificial additives with purification. (a) Thermogravimetric analysis (TGA) showing thermolysis of artificial additives. (b,c) Illustration of water solubility of artificial additives with or without purification after placement three months. (d) Demonstration of calligraphy using artificial additives as ink.

Figure S1 illustrates the TGA results of characterization with or without purification, showing the densities of SWCNT1@LGS and MWCNT1@LGS increased in comparison to those of unpurified treatment. Thus, purification strategy contributes to high density and enhancing the utilization of CNTs in novel feeding additives by removing excessive LGS wrapping. We also found that the water solubility of these additives is different. Pristine CNTs are difficult to disperse in a drop, while purified CNTs disperse to form a colorless drop, and unpurified CNTs disperse to form a yellow drop with excess LGS. In order to further show these differences, we used examples of calligraphy with Chinese characters of Xi'an Jiaotong University to demonstrate the effects of water solubility and color justification.

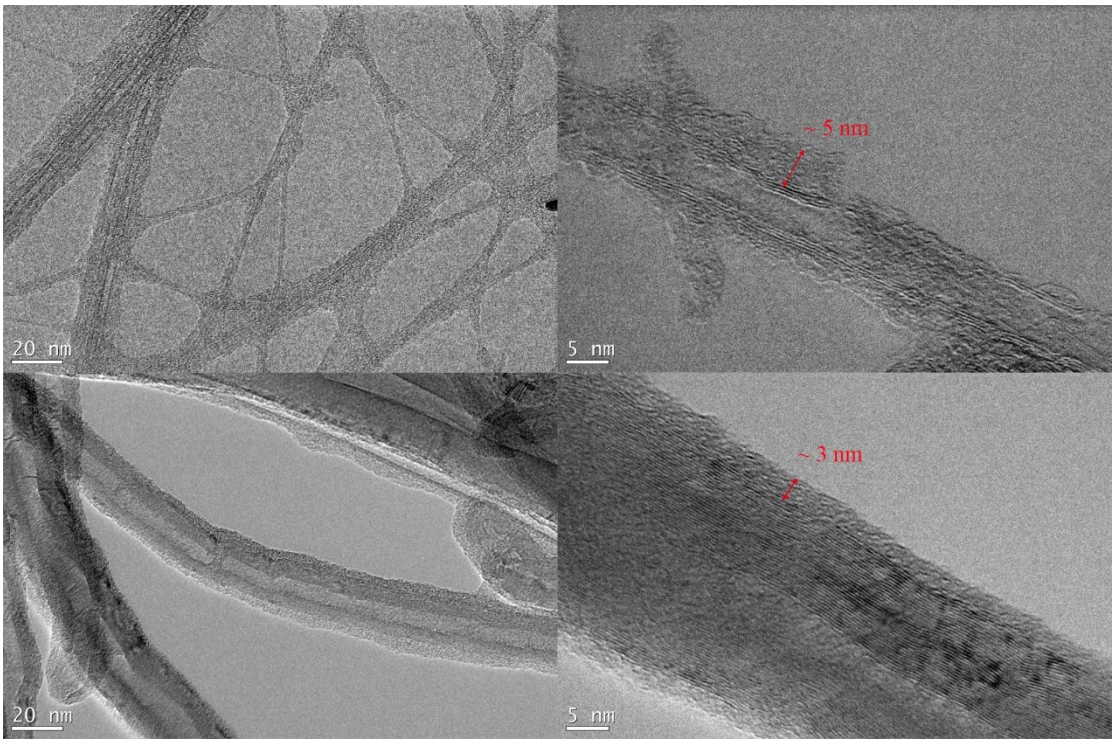

Figure S2. High-resolution Transmission Electron Microscopy (HR-TEM) images of artificial additives. On top pictures the left shows the composite of SWCNT@LGS formation, and the right gives direct observation of SWCNTs wrapped by LGS. On the bottom, similar pictures with the left showing the composite of MWCNT@LGS formation and the right giving direct view of MWCNTs coated by LGS.

Figure S2 exhibits nanoscale views of SWCNTs and MWCNTs wrapped by LGS. From the top and bottom pictures, we can estimate that the coatings were about 5 nm and 3 nm, respectively, because of the use of LGS with molecular weight of 10,000. This situation shows that the CNTs, with biocompatibility, formed.

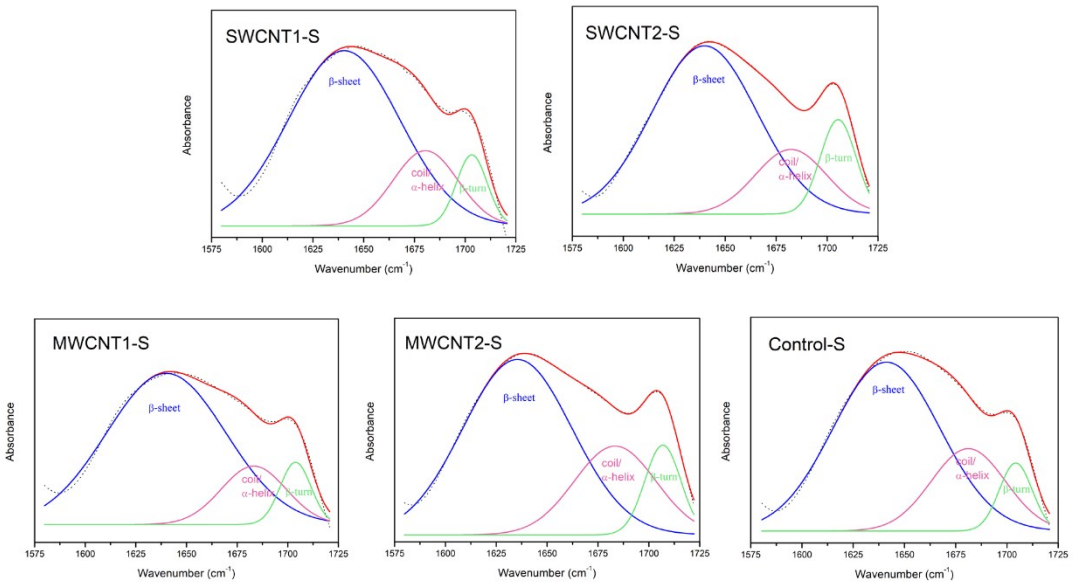

Figure S3. The deconvoluted peaks of Amide I FTIR spectra in range from 1575 cm^{-1} to 1725 cm^{-1} with blue solid line as β-sheet, pink red solid line as random coil or α-helix, and light green solid line as β-turn (three smooth Gaussian curves) according to black dotted line as raw spectra and red solid line as fitted curves.

Figure S3 shows deconvoluted FTIR spectra for five silk samples including SWCNT1-S, SWCNT2-S, MWCNT1-S, MWCNT2-S, Control-S. The Origin pro 8 analytical software was used to be in range from 1575 cm^{-1} to 1725 cm^{-1} for each Amide I spectrum by a second-order Savitzky-Golay method for smooth curves and by the Gaussian method for fitting simulation. On the basis of black dotted line for raw spectra and red solid line for fitted curves, we obtained three Gaussian smooth curves including blue solid line for β-sheet, pink red solid line for random coil or α-helix, and light green solid line for β-turn. The statistical data with Lambert Beer's law were presented in Table S1.

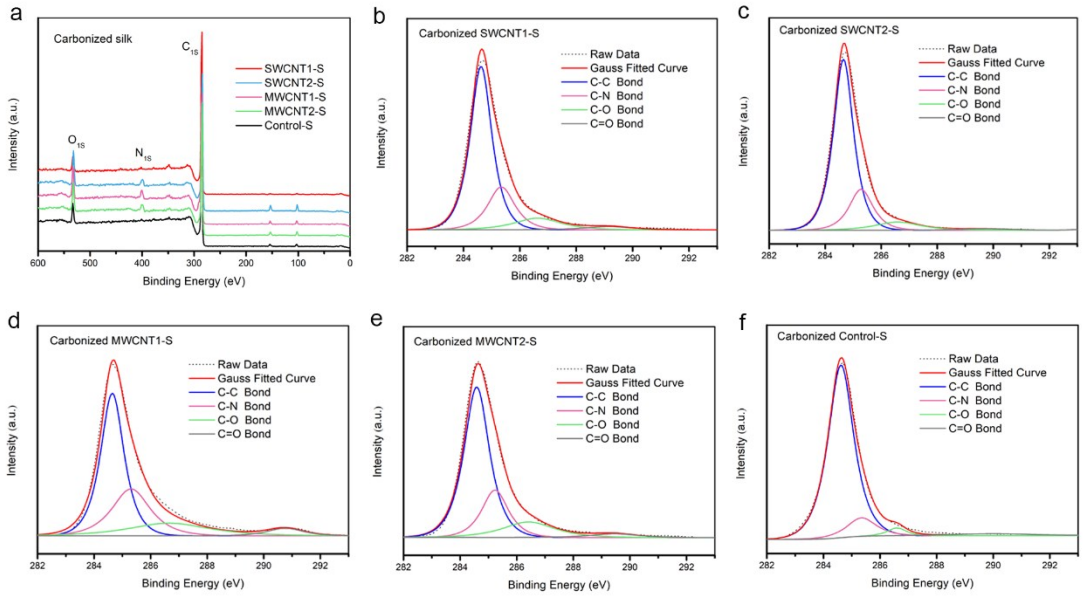

Figure S4. The XPS survey spectra and the deconvoluted peaks of C1s spectra for carbonized silk fibers. (a) XPS survey spectra of the carbonized silks and (b-f) high-resolution peaks of C1s spectra for carbonized silks.

Figure S4 shows the XPS spectra of carbonized silks and the deconvolutions of C1s XPS peaks for carbonized silks according to atomic content of C-C bonds, C-N bonds, C-O bonds, and C=O bonds, respectively. We used XPS-AVANTAGE software to correct and decompose their spectral peaks, and simulate Gaussian curves for atomic components. The deconvoluted peaks of C1s XPS spectra from 282 eV to 293 eV with blue solid line for C-C bonds, pink red solid line for C-N bonds, light green solid line for C-O bonds, and gray solid line for C=O bonds (four smooth Gaussian curves) according to the black dotted line as raw data and the red solid line as the sum of the Gaussian fitted curves. The results are shown in Table S2.

Pristine diameters of five silk samples including Control-S, SWCNT1-S, SWCNT2-S, MWCNT1-S, MWCNT2-S, respectively. More than forty degummed single silk fibers in each group were measured for an average diameter, as showed in Table S3.

Experimental parameters of mechanical properties, including stress at fracture, strain at fracture, and toughness modulus. Note that the toughness modulus can be defined as the area under the stress-strain curve. We used Origin pro 8 to directly calculate the areas. A total 50 *B. mori* silkworms were naturally fed in a self-adjustive rearing-box, and a total of 20 silk samples (two silk fibers randomly selected from each cocoon, ten cocoons for each group) for each group were measured to obtain the average data and standard deviations. The detailed data are shown in Tables S4-S8.

Carbonized silks possess electrical conductivity resulting from the high crystallinity of graphitization. We used a tube-furnace under Ar atmosphere to heat silk fibers from room temperature to 350°C. After holding at 350°C for 2.5 hours, the temperature was increased from 350°C to 900°C and held again for 2 hours to form the conjugated hexagonal rings of graphitization. The details are shown in Table S9. Before conductivity measurement, error bars were obtained from the test device without any carbonized samples. For each measurement, the conductivity was characterized by digital multimeter to obtain the resistance, which was converted to conductivity according to Equation (1), (2) and Diagrammatic sketch (3) below:

$$\Delta R = \rho * \frac{\Delta L}{S}$$ **Equation (1)**

$$\sigma = \frac{1}{\rho}$$ **Equation (2)**

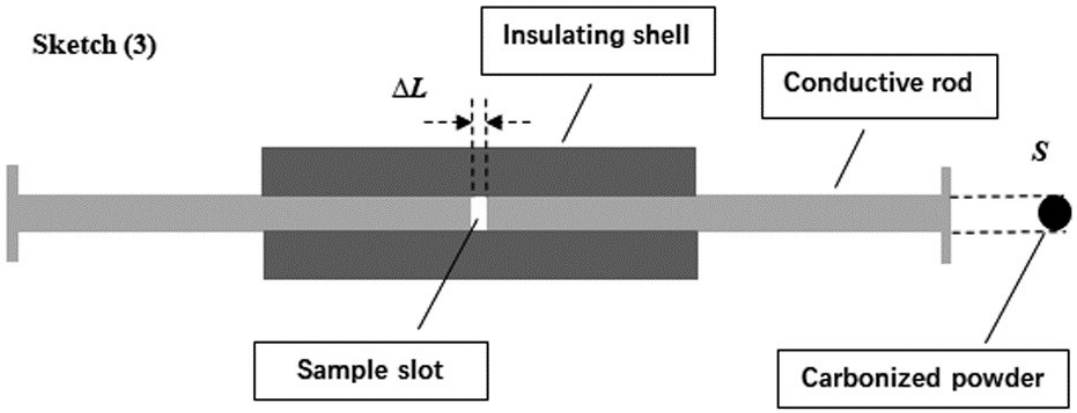

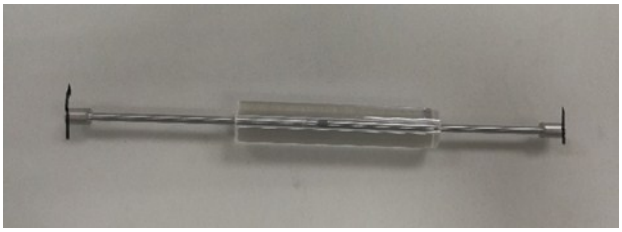

Figure S5. The test device of electrical conductivity. This device includes cylindrical insulating shell and two conductive rods, which are pulled out from the shell. Sample can be added in the narrow slot and compacted flat to measure the resistance by digital multimeter.

2. Supplementary Tables S1-S10

Table S1. Secondary structural contents in Amide I of degummed silk fibers

Silk samples	β-sheet content (%)	Random coil/α-helix content (%)	β-turn content (%)
SWCNT1-S	73.28	18.47	8.24
SWCNT2-S	69.19	18.00	12.83
MWCNT1-S	75.69	16.13	8.18
MWCNT2-S	64.95	24.34	10.67
Control-S	68.59	22.61	8.42

Table S2. Atomic content (%) of carbonized silks based on C1s spectrum

	SWCNT1-S	SWCNT2-S	MWCNT1-S	MWCNT2-S	Control-S
C-C	65.69	70.92	52.4	63.09	83.82
C-N	19.94	21.3	20.73	27.87	10.22
C-O	7.57	10.07	13.21	15.61	2.9
C=O	1.57	2.93	2.96	4.12	3.07

Table S3. Average Diameter of Degummed Silk Fibers

silk samples	average diameter [μm]
Control-S	11.50±0.64
SWCNT1-S	11.37±0.58
SWCNT2-S	11.46±0.49
MWCNT1-S	11.24±0.69
MWCNT2-S	11.28±0.78

Table S4. Mechanical Properties of Degummed Control-S Fibers

cocoon #	stress at fracture [GPa]	strain at fracture [%]	toughness modulus [MPa]
1	0.65	11.13	48.55
2	0.70	9.50	43.34
3	0.67	8.99	37.08
4	0.60	10.44	39.16
5	0.51	15.40	57.15
6	0.64	13.01	50.01
7	0.52	16.08	53.92
8	0.61	14.77	51.07
9	0.59	11.70	42.41
10	0.54	15.73	56.37
average	0.60	12.67	47.90
standard deviation	0.06	2.68	7.09

Table S5. Mechanical Properties of Degummed SWCNT1-S Fibers

cocoon #	stress at fracture [GPa]	strain at fracture [%]	toughness modulus [MPa]
1	0.99	14.25	88.28
2	0.89	10.64	70.70
3	0.84	12.18	63.51
4	1.01	9.95	60.58
5	0.80	13.64	63.95
6	0.93	12.35	68.48
7	0.81	13.33	65.80
8	0.84	12.88	66.56
9	0.86	11.23	61.84
10	0.84	13.90	73.36
average	0.88	12.43	68.30
standard deviation	0.07	1.45	8.05

Table S6. Mechanical Properties of Degummed SWCNT2-S Fibers

cocoon #	stress at fracture [GPa]	strain at fracture [%]	toughness modulus [MPa]
1	0.52	13.71	41.83
2	0.69	11.37	45.12
3	0.58	12.73	48.81
4	0.50	14.74	40.63
5	0.79	10.44	48.66
6	0.80	19.73	96.52
7	0.76	14.04	67.81
8	0.64	16.29	68.97
9	0.81	19.00	102.37
10	0.82	15.25	79.34
average	0.69	14.73	64.00
standard deviation	0.12	3.00	22.77

Table S7. Mechanical Properties of Degummed MWCNT1-S Fibers

cocoon #	stress at fracture [GPa]	strain at fracture [%]	toughness modulus [MPa]
1	1.18	18.30	147.09
2	1.34	18.63	154.03
3	1.13	14.35	102.30
4	0.99	18.50	117.89
5	0.83	13.08	77.67
6	0.94	18.45	107.00
7	1.06	18.60	126.55
8	1.17	14.10	92.77
9	0.88	17.58	98.59
10	1.19	16.40	108.48
average	1.07	16.80	113.23
standard deviation	0.16	2.17	23.78

Table S8. Mechanical Properties of Degummed MWCNT2-S Fibers

cocoon #	stress at fracture [GPa]	strain at fracture [%]	toughness modulus [MPa]
1	0.92	15.18	90.36
2	0.88	17.85	94.81
3	0.75	21.65	99.94
4	0.68	14.20	57.64
5	0.85	13.40	66.31
6	0.77	11.35	53.16
7	0.77	12.55	52.41
8	0.76	11.80	52.15
9	0.70	12.05	53.96
10	0.73	11.80	46.30
average	0.78	14.18	66.70
standard deviation	0.08	3.29	20.31

Table S9. Electrical Conductivity of Graphitized Silk Fibers

	R_0 (Ω)= 0.7	L_0 (cm)= 12.144	S (cm^2)= 0.0314		
silk samples	R (Ω)	ΔR (Ω)	L (cm)	ΔL (cm)	σ (S/cm)
SWCNT1-S	2.2	1.5	12.233	0.089	1.89±0.05
SWCNT2-S	3.2	2.5	12.259	0.115	1.46±0.05
MWCNT1-S	2.9	2.2	12.284	0.140	2.03±0.05
MWCNT2-S	3.6	2.9	12.270	0.126	1.38±0.05
Control-S	3.2	2.5	12.259	0.114	1.45±0.05

Table S10. Tensile toughness of spider and silkworm silk fiber

Silk types	Stress at fracture (GPa)	Strain at fracture (%)	Toughness modulus (GJ m^{-3})	Ref.
Araneus diadematus (MA spider silk)	1.20	27.00	0.16	[S1]
Pholcus opilionoides (spider silk-SWNT-2)	5.39	75.00	2.14	[S2]
Nephila edulis (spider dragline silk)	0.80	25.00	/	[S3]
Bombyx mori (silkworm cocoon silk)	0.40	22.00	/	[S3]
Bombyx mori (silk reeled at 27 mm/s)	0.90	18.00	/	[S4]
Bombyx mori (silk-purified-MWNT1)	1.07	16.80	11.32	**This work**
Bombyx mori (silk-pufrified-SWNT1)	0.88	12.43	6.83	**This work**
Bombyx mori (silk-SWNT1)	0.59	12.59	4.82	[S5]
Bombyx mori (silk-GR1)	0.57	10.33	3.80	[S5]
Bombyx mori (silk-MWNT)	1.69	24.00	0.38	[S6]

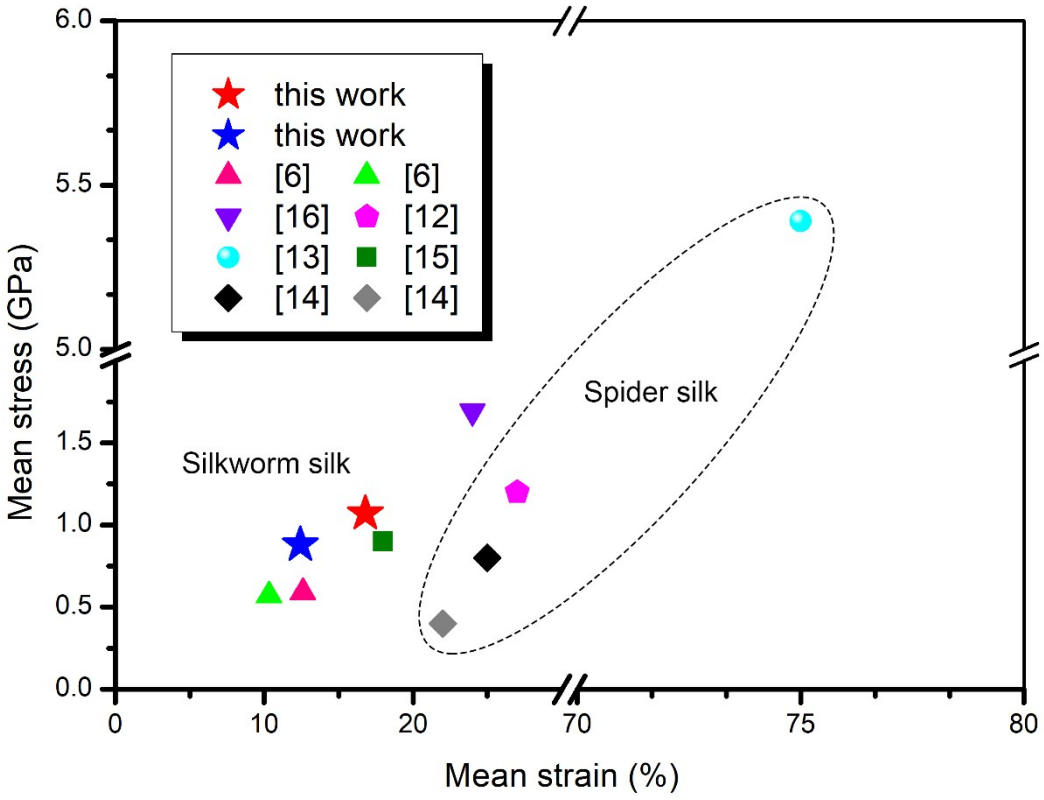

Figure S6. Schematic reference for strength-at-fracture of spider or silkworm silk.

References

[S1] J.M. Gosline, P.A. Guerette, C.S. Ortlepp, K.N. Savage The mechanical design of spider silks: from fibroin sequence to mechanical function. J. Exp. Biol. 1999, Pt 23(*202*):3295-3303.

[S2] E. Lepore, F. Bosia, F. Bonaccorso, M. Bruna, S. Taioli Spider silk reinforced by graphene or carbon nanotubes. 2D Mater. 2017,(*4*):31013.

[S3] J. Sirichaisit, V.L. Brookes, R.J. Young, F. Vollrath Analysis of Structure/Property Relationships in Silkworm (Bombyx mori) and Spider Dragline (Nephila edulis) Silks Using Raman Spectroscopy. Biomacromolecules 2003, 2(*4*):387-394.

[S4] Z. Shao, F. Vollrath Surprising strength of silkworm silk. Nature 2002,(*418*):741.

[S5] Q. Wang, C. Wang, M. Zhang, M. Jian, Y. Zhang Feeding Single-Walled Carbon Nanotubes or Graphene to Silkworms for Reinforced Silk Fibers. Nano Lett. 2016,(*16*):6695-6700.

[S6] J.T. Wang, L.L. Li, M.Y. Zhang, S.L. Liu, L.H. Jiang Directly obtaining high strength silk fiber from silkworm by feeding carbon nanotubes. Mater. Sci. Eng., C 2014,(*34*):417-421.